Squeezed Condensates

submitted to Phys. Rev. A

Uffe V. Poulsen and Klaus Mølmer
Institute of Physics and Astronomy, University of Aarhus, DK-8000 Århus C, Denmark
email: uvp@ifa.au.dk

February 1, 2008

Abstract

We analyse the atomic state obtained by photo-dissociation of a molecular Bose-Einstein-condensate. This process is equivalent to down-conversion in quantum optics where it is responsible for squeezing of the field amplitudes. Monte Carlo simulations derived from the Positive P description of the system, and approximate equations for second moments of the atomic field operators are introduced to describe the early stages of the process – not amenable to the usual mean-field description.

1 Introduction

Like electromagnetic waves, atomic matter waves can to a large extent be manipulated in space. Interference phenomena have been observed, and a large number of high precision atom optics measurements have been carried out [1]. One of the potential future applications of atomic Bose-Einstein condensates is as coherent matter wave sources for interferometric time and frequency standards, detection of inertial effects, and a host of related technological tasks. The spatial [2] and temporal [3] coherence of condensates has been verified, and coherent amplification of matter waves has been demonstrated [4] to establish the close analogy with laser and maser sources of light.

For high precision purposes, however, it was realized long time ago, that so-called non-classical states of light may be more useful than classical field states [5]. It is therefore natural to consider the production of such 'non-classical' states of atoms as well. The term 'non-classical' is ambiguous here, since what is very non-classical for light, *e.g.* a number state, can seem perfectly classical for atoms, and we shall instead use the term quantum correlated states. Due to the collisional interaction between atoms in a Bose condensate, this system contains a non-linearity, in equivalence with the Kerr-effect for light, and this collisional interaction has already been observed [6] in a matter wave analog of four-wave mixing in non-linear optics. There have been several proposals to utilize collisional effects to produce certain quantum correlated states, such as Schrödinger cat-like states [7], and to observe the effect of the non-linearity on the dynamics of the condensate [8]. It is clear from these studies that, even though the collisional interaction can be controlled experimentally [9] it is not easy to control precisely the quantum features of interest; the problem is a genuine multi-mode one due to the spatial degrees of freedom, and one has to pay attention to the role of non-condensed atoms, as well.

In this Paper, we suggest to follow instead the procedure of quantum optics for production of squeezed light: we suggest to implement an 'atomic OPO'. The optical parametric oscillator (OPO) is a device where light is down converted, so that a single pump photon at frequency 2ω is converted into two photons, each of frequency ω (degenerate case). The process is the inverse of second harmonic generation (SHG), and in practical experiments, one often sees a strong field of frequency ω, which is first frequency doubled in the SHG crystal, and the high frequency field is subsequently down-converted in a similar non-linear crystal, now working as an OPO.

The matter wave analogue of the SHG process is one in which the atoms are combined by photo-association into di-atomic molecules. This process has been analyzed theoretically [10], and it was recently demonstrated experimentally, that part of an atomic condensate may be converted by stimulated Raman transitions into molecules this way [11]. We suggest to follow the analogy with the OPO quite directly, *i.e.*, to apply laser fields to drive the Raman transition from the molecular state back to free atoms (photo-dissociation), and we note, that the quantum correlations appear due to the fact that only even number states for the atomic component will be present in the sample, because atoms are created in pairs.

The dynamics of coupled atomic and molecular degenerate gasses has been studied in some detail [12] with particular focus on the spatial and temporal dependence of the mean field dynamics, *e.g.*, the appearance of solitons [13]. We focus on the "quantum optics" aspects, *i.e.*, the atom number distribution, and the consequences for atom counting experiments.

The organization of this paper is as follows: In Sec. 2, we present our proposal, and we derive two theoretical methods, one approximate and one exact, to analyze the dynamics of the system. In Sec. 3 we present numerical results for various relevant quantities. In Sec. 4 we analyze the use of our quantum correlated atoms as squeezed input in two-state Rabi-oscillations with a large, "classical", condensate. In Sec. 5, we discuss the results and we briefly indicate some alternative ideas for the production and application of quantum correlated condensates.

2 The model

2.1 Trapped cold atoms in second quantization

It is convenient to describe dilute gasses of cold atoms in a trap in the second quantized formalism. In this description the Hamiltonian for the system at low temperatures is usually taken to be:

$$H_0^{3\mathrm{D}} = \int d\vec{r} \left\{ \hat{\psi}^\dagger(\vec{r}) h_1 \hat{\psi}(\vec{r}) + \frac{g}{2} \hat{\psi}^\dagger(\vec{r}) \hat{\psi}^\dagger(\vec{r}) \hat{\psi}(\vec{r}) \hat{\psi}(\vec{r}) \right\}. \tag{1}$$

The atomic field operators $\hat{\psi}(\vec{r})$ and $\hat{\psi}^\dagger(\vec{r})$ annihilate and create an atom at position $\vec{r}$ and they satisfy the equal time commutation relations

$$\left[\hat{\psi}(\vec{r}), \hat{\psi}^\dagger(\vec{r}') \right] = \delta^3(\vec{r} - \vec{r}') \tag{2}$$

The single particle Hamiltonian h_1 is the one appropriate for a single atom of mass m in the external trapping potential V_{ext}

$$h_1 = -\frac{\hbar^2}{2m} \vec{\nabla}^2 + V_{ext}(\vec{r}). \tag{3}$$

The g term in Eq.(1) describes the collisional two body interaction of the atoms. The simple contact form is an approximation appropriate for cold, dilute gases [14]. The value of the strength parameter is $g = 4\pi\hbar a_s/m$ where a_s is the s-wave scattering length.

In most experiments the trapping potential can be approximated well by a three dimensional harmonic oscillator characterized by three frequencies ω_x, ω_y and ω_z. If one of these frequencies is significantly smaller than the other two the atoms will form an elongated cloud and we describe such an effectively one dimensional system by a single frequency ω [15].

We shall work with dimensionless equations and choose to measure time in units of ω^{-1}, lengths in units of $a_0 = \sqrt{\hbar/\omega m}$, and energy in units of $\hbar\omega$. We are then left with

$$H_0 = \int dx \left\{ \hat{\psi}^\dagger(x) h_1 \hat{\psi}(x) + \frac{g}{2} \hat{\psi}^\dagger(x) \hat{\psi}^\dagger(x) \hat{\psi}(x) \hat{\psi}(x) \right\} \tag{4}$$

where

$$h_1 = -\frac{1}{2} \frac{\partial^2}{\partial x^2} + \frac{1}{2} x^2. \tag{5}$$

and where $g = 4\pi a_s/a_0$ is a dimensionally correct, one dimensional interaction strength [16].

2.2 Photodissociation from a molecular condensate

Starting from a molecular condensate (prepared by photo-association or by other means) we can imagine to photo-dissociate or "down convert" the molecules to pairs of free atoms. A suitable Hamiltonian to describe photo-dissociation is

$$H_{PD} = \frac{1}{2}\int dx\ \left\{ b(x,x',t)\hat{\psi}^\dagger(x)\hat{\psi}^\dagger(x') + b^*(x,x',t)\hat{\psi}(x)\hat{\psi}(x') \right\}. \tag{6}$$

This Hamiltonian clearly creates and annihilates atoms in pairs. A full description should also include the molecules such that each atomic pair creation would be accompanied by the annihilation of a molecule. Here we will assume the molecular condensate to be large and the number of molecules removed to be small. In that case it is reasonable to describe the molecular condensate by a time-independent c-number field. The function b in Eq.(6) is the product of this field and of the coupling to a position dependent laser field which is also assumed to be classical. To represent the position dependence of the molecular condensate and of the laser field, the relative wavefunction of the pair of atoms, and the time dependence of the laser field, we use the ansatz

$$b(x,x',t) = \frac{B}{2\pi\sigma_r\sigma_{cm}} \exp\left(-2i\Delta t\right) \exp\left(-\frac{1}{2}\frac{(x-x')^2}{\sigma_r^2}\right) \exp\left(-\frac{1}{2}\frac{(\frac{1}{2}(x+x'))^2}{\sigma_{cm}^2}\right) \tag{7}$$

where $\sigma_r \ll \sigma_{cm} \cong a_0$.

2.3 Operator equations of motion

A successful tool for the description of a Bose condensate is the Gross-Pitaevskii equation (GPE). It can be obtained from the Heisenberg equation of motion for the atomic field $\hat{\psi}(x,t)$ by taking average values and by replacing the mean value of an operator product by the product of mean values. In our case the Heisenberg equation reads:

$$i\frac{\partial\hat{\psi}(x,t)}{\partial t} = \left(-\frac{1}{2}\frac{\partial}{\partial x} + \frac{1}{2}x^2 + g\hat{\psi}^\dagger(x,t)\hat{\psi}(x,t)\right)\hat{\psi}(x,t) + \int dx'\ b(x,x',t)\hat{\psi}^\dagger(x',t). \tag{8}$$

The last term in this equation is due to the exchange of atom pairs with the molecular condensate *via* photo-dissociation.

It is easy to see that using the average of Eq.(8) has shortcomings when we try to describe photo-dissociation: If we start from the atomic vacuum defined by

$$\hat{\psi}(x,0)|0\rangle \quad = \quad 0 \tag{9}$$

the incoupling term on the right hand side has vanishing average value. Therefore $\langle\hat{\psi}(x,t)\rangle$ will stay zero also at all later times and no useful information can be extracted.

To gain knowledge of the state created we therefore proceed to study expressions quadratic in the field operators. To shorten notation we define

$$\hat{R}(x,y,t) \quad \equiv \quad \hat{\psi}^\dagger(x,t)\hat{\psi}(y,t) \tag{10}$$

$$\hat{S}(x,y,t) \quad \equiv \quad \hat{\psi}(x,t)\hat{\psi}(y,t). \tag{11}$$

For these operators we get the following Heisenberg equations of motion:

$$\begin{aligned} i\frac{\partial\hat{R}(x,y,t)}{\partial t} \quad = \quad & \left(\frac{1}{2}\frac{\partial^2}{\partial x^2} - \frac{1}{2}x^2 - \frac{1}{2}\frac{\partial^2}{\partial y^2} + \frac{1}{2}y^2\right)\hat{R}(x,y,t) \\ & + g\left(\hat{R}(y,y,t) - \hat{R}(x,x,t)\right)\hat{R}(x,y,t) \\ & + \int dz\ \left\{ b(z,y,t)\hat{S}^\dagger(x,z,t) - b^*(x,z,t)\hat{S}(z,y,t) \right\} \end{aligned} \tag{12}$$

and

$$
\begin{aligned}
i\frac{\partial \hat{S}(x,y,t)}{\partial t} &= \left(-\frac{1}{2}\frac{\partial^2}{\partial x^2}+\frac{1}{2}x^2-\frac{1}{2}\frac{\partial^2}{\partial y^2}+\frac{1}{2}y^2\right)\hat{S}(x,y,t) \\
&\quad +g\left(\delta(x-y)+\hat{R}(x,x,t)+\hat{R}(y,y,t)\right)\hat{S}(x,y,t) \\
&\quad +\int dz\ \left\{b(z,y,t)\hat{R}(z,x)+b(x,z,t)\hat{R}(z,y)\right\}+b(x,y,t). \qquad (13)
\end{aligned}
$$

Note that $b(x,y,t)$ now appears as an inhomogeneous source term in the $\hat{S}$ equation. This guarantees a nontrivial behaviour when we take averages. Note also that when taking averages we have a problem with the interaction terms which will couple the second order expectations to fourth order expectations. These fourth order terms have to be factorized in some approximate way to obtain a closed set of equations.

2.4 c-number equations

2.4.1 Exact equations for $g = 0$

When $g = 0$, Eq.(12) and Eq.(13) can be reduced to two coupled linear equations for the moments

$$
R(x,y,t) \equiv \langle \hat{R}(x,y,t)\rangle \quad , \quad S(x,y,t) \equiv \langle \hat{S}(x,y,t)\rangle. \qquad (14)
$$

They read:

$$
\begin{aligned}
i\frac{\partial R(x,y,t)}{\partial t} &= \left(\frac{1}{2}\frac{\partial^2}{\partial x^2}-\frac{1}{2}x^2-\frac{1}{2}\frac{\partial^2}{\partial y^2}+\frac{1}{2}y^2\right)R(x,y,t) \\
&\quad +\int dz\ \{b(z,y,t)S^*(x,z,t)-b^*(x,z,t)S(z,y,t)\} \qquad (15) \\
i\frac{\partial S(x,y,t)}{\partial t} &= \left(-\frac{1}{2}\frac{\partial^2}{\partial x^2}+\frac{1}{2}x^2-\frac{1}{2}\frac{\partial^2}{\partial y^2}+\frac{1}{2}y^2\right)S(x,y,t) \\
&\quad +\int dz\ \{b(z,y,t)R(z,x)+b(x,z,t)R(z,y)\} \\
&\quad +b(x,y,t). \qquad (16)
\end{aligned}
$$

Moreover, R and S uniquely determine all higher order expectation values. This can be seen in a number of ways. One is to note that the Wigner distribution is a multi-dimensional gaussian distribution fully characterized by its second order moments [17, 18]. Another follows from the observation that when $g = 0$, the Heisenberg equation of motion (8) implies that $\hat{\psi}(x,t)$ can at all times be expressed as a linear combination of the initial values

$$
\hat{\psi}(x,t) = \int dy\ \left\{f(x,y,t)\hat{\psi}(y,0)+g(x,y,t)\hat{\psi}^\dagger(y,0)\right\}. \qquad (17)
$$

Eq.(17), its hermitian conjugate and the fact that our system starts in the vacuum state then suggest the following scheme for calculation of any operator product at arbritrary t: Use the commutation relation (2) to move all $\hat{\psi}(x,0)$ to the right of any $\hat{\psi}^\dagger(y,0)$ (normal ordering). Of all the terms produced in this process only the ones consisting entirely of c-numbers are nonzero as the vacuum expectation of any normal ordered product of operators vanishes in the vacuum state. To evalute the c-number terms we formally need to calculate integrals of products of the f and g functions of Eq.(17). It is, however, not difficult to see that these integrals factorize and that the factors are exactly the ones involved in calculating expectation values of products of only two field operators. The end result is that the average of any operator product is replaced by a sum of all possible factorizations into two-operator expectations

$$
\begin{aligned}
\langle\hat{\psi}^\dagger(x_1)\hat{\psi}^\dagger(x_2)\hat{\psi}(x_3)\hat{\psi}(x_4)\rangle &= \langle\hat{\psi}^\dagger(x_1)\hat{\psi}^\dagger(x_2)\rangle\langle\hat{\psi}(x_3)\hat{\psi}(x_4)\rangle \\
&\quad +\langle\hat{\psi}^\dagger(x_1)\hat{\psi}(x_3)\rangle\langle\hat{\psi}^\dagger(x_2)\hat{\psi}(x_4)\rangle \\
&\quad +\langle\hat{\psi}^\dagger(x_1)\hat{\psi}(x_4)\rangle\langle\hat{\psi}^\dagger(x_2)\hat{\psi}(x_3)\rangle. \qquad (18)
\end{aligned}
$$

This is a simple version of Wick's theorem [19].

2.4.2 Approximate equations for $g \neq 0$

When $g \neq 0$ we have to include the interaction term of Eqs.(12,13) in Eqs.(15,16). Unfortunately, the decomposition Eq.(17) is no longer exact, and there is no simple way to reduce the mean values of four-operator products to products of R and S. Rather than the simple replacement, *e.g.*, $\hat{R}(y,y)\hat{R}(x,y) \to R(y,y)R(x,y)$, we choose to apply the Wick prescription as this is correct to lowest order. We then get

$$\begin{aligned} g\left\langle \hat{R}(y,y,t)\hat{R}(x,y,t) - \hat{R}(x,x,t)\hat{R}(x,y,t)\right\rangle &\to g\left(S^*(x,y,t)S(y,y,t) - S(x,y,t)S^*(x,x,t)\right) \\ &\quad +2g\left(R(y,y,t) - R(x,x,t)\right)R(x,y,t) \qquad (19) \\ g\left\langle \left(\hat{R}(x,x,t) + \hat{R}(y,y,t) + \delta(x-y)\right)\hat{S}(x,y,t)\right\rangle &\to 2g\left(R(y,y,t) + R(x,x,t)\right)S(x,y,t) \\ &\quad +g\left(R(x,y,t)S(x,x,t) + R^*(x,y,t)S(y,y,t)\right) \\ &\quad +g\delta(x-y)S(x,y,t) \qquad (20) \end{aligned}$$

When these expressions are inserted into Eqs.(15,16), we arrive at the equations we want to solve numerically. We use a split-step approach where the kinetic energy is treated by a Fourier method. The remaining terms are dealt with by a fourth order Runge-Kutta scheme. In this one-dimensional problem the equations are quite manageable.

2.5 The positive P pseudo-probability distribution

Pseudo-probablity distributions (PPD's) are well-established tools in quantum mechanics. The most well known of the distributions are the Glauber-Sudarshan P-function and the Wigner function but especially in quantum optics a number of other distributions have also been useful. Common to all the PPD's is that they provide the expectation values of properly ordered operator products as weighted c-number averages. The *positive P distribution* [18, 15, 20] (P_+) that we will be using here gives the expection values of normally ordered products by replacing $\hat{\psi}$ by a c-number function ψ_1 and $\hat{\psi}^\dagger$ by a c-number function ψ_2, *e.g.*:

$$\langle \hat{\psi}^\dagger(x,t)\hat{\psi}(y,t)\rangle = \int d[\psi_1]d[\psi_2]\psi_2(x)\psi_1(y)P_+[\psi_1,\psi_2,t]. \qquad (21)$$

Note that P_+ is the joint distribution of two spatial functions and it is therefore an immensely complicated functional in general. It satisfies a multi-dimensional Fokker-Planck equation which, however, opens the door to a Monte Carlo sampling as we can translate the Fokker-Planck equation for the distribution to Langevin equations for stochastic realizations of $\psi_1(x,t)$ and $\psi_2(x,t)$. These equations resemble the GPE but they are coupled and they contain noise terms. A derivation of the equations without incoupling is given in [15] (see also [21]) and the inclusion of incoupling is straightforward. In the notation of stochastic differential equations the equations can be written

$$\begin{aligned} id\psi_1(x) &= \left(h_1\psi_1(x) + g\psi_2(x)\psi_1(x)\psi_1(x)\right)dt \qquad (22) \\ &\quad + \int b(x,x')\psi_2(x')dx' + dW_1(x) \qquad (23) \\ -id\psi_2(x) &= \left(h_1\psi_2(x) + g\psi_1(x)\psi_2(x)\psi_2(x)\right)dt \qquad (24) \\ &\quad + \int b^*(x,x')\psi_1(x')dx' + dW_2(x) \qquad (25) \end{aligned}$$

where h_1 is still defined in Eq.(3) and the noise terms are gaussian and given by

$$\begin{aligned} \langle dW_{1,2}(x,t)\rangle &= 0 \qquad (26) \\ \langle dW_1(x,t)dW_2(x',t')\rangle &= 0 \qquad (27) \\ \langle dW_1(x,t)dW_1(x',t')\rangle &= idt\left(b(x,x',t) + g\psi_1(x,t)\delta(x-x')\right)\delta(t-t') \qquad (28) \\ \langle dW_2(x,t)dW_2(x',t')\rangle &= -idt\left(b^*(x,x',t) + g\psi_1(x,t)\delta(x-x')\right)\delta(t-t'). \qquad (29) \end{aligned}$$

By numerically simulating Eqs.(23,25) we are able to calculate expectation values of arbitrary, normally ordered field operator products with the only approximation that the results are subject to sampling errors due to the use of finite ensembles. We describe in the appendix our procedure to synthesize the noise dW in our simulations.

The crucial drawback of the method is the well know sudden divergence in some of the unphysical moments of the P_+ distribution[21, 22]. Unphysical moments exist because the translation from operator products to products of ψ_1 and ψ_2 never involves ψ_1^* and ψ_2^*. This leaves some room for P_+ to behave badly and unfortunately it exploits this freedom. In the wavefunction realizations, some wavefunctions diverge or they make very large excursions that are difficult to follow numerically and which make a devastating impact on the sampling error. The P_+ Monte Carlo method is therefore limited to short times where only few atoms have been created and nonlinear effects are still small. This suits our purpose, since we are only interested in short time dynamics, and we shall trust the result produced by the Langevin equations as long as none of the wavefunctions in the ensemble have escaped the region where we have confidence in our integration algorithm.

3 Results

In this section we show results for some of the quantities of interest that we are able to calculate in our model. Although the main new feature lie in the quantum correlations we first show a very classical quantity, namely the density profile. We then proceed to look at the eigenvalues of the one-particle density matrix. The largest of these eigenvalues defines the condensate fraction and the corresponding eigenvector is the condensate wavefunction. Finally we turn to a two-body quantity, the second order correlation function.

3.1 The density profile and the number of atoms

The atomic density is given by the diagonal elements of the one-body density operator in the position representation, that is

$$\rho(x,x) = \langle \hat{\psi}^\dagger(x)\hat{\psi}(x)\rangle = R(x,x) = \overline{\psi_2(x)\psi_1(x)}, \tag{30}$$

where the overbar in the last expression denotes the average over many realizations of the stochastic $\psi_1(x,t)$ and $\psi_2(x,t)$. In Fig. 1 is shown a typical plot of this profile at $\omega t = 2.4$. It has the characteristic gaussian shape of the harmonic oscillator ground state and as we shall see in Sec. 3.2 a large fraction of the atoms indeed occupy a common wavefunction close to this state. The R&S equations (15,16) with the interaction terms (19,20) give results in excellent agreement with the P_+ simulations.

The total number of photo-dissociated atoms is obtained as the trace of the one-body density-operator or, according to Eq.(30), simply as

$$N = \int dx\ \rho(x,x). \tag{31}$$

In Fig. 2 this number is shown as a function of time for $g = 0$ and for $g = 0.01$. The agreement between the R&S equations and the P_+ method is seen to be quite good.

3.2 The condensate fraction and wavefunction

By diagonalizing the one-body density matrix we obtain an orthonormal basis of single-particle states. The eigenvalues correspond to the populations of these states and in the case of a condensate one of these eigenvalues dominates, *i.e.*, most particles occupy the same state. A dynamical picture of the condensation process is the Bose-enhancement of the scattering into the most occupied state. Here we expect a similar effect to take place. At first several states of the system are occupied by the atoms created. As the number of atoms grows the stimulated character of the

creation becomes more important and a mode competition results in one mode being preferentially occupied.

In Fig.3 we show the condensate fraction, *i.e.* the ratio of the largest eigenvalue of the one-body density matrix to the sum of the eigenvalues for different values of the interaction strenght g. It is seen that as expected the condensate fraction is in general an increasing function of time. The effects of interactions are rather small at these low atom numbers. Note that unlike studies of stationary condensates at $T = 0$, where interactions are responsible for the breakdown of a simple product state ansatz for the system and the existence of atoms outside the condensate, our incoupling by itself produces atoms both in the condensate and outside the condensate. In fact, our calculations show that the second-largest eigenvalue accounts for most of the atoms which are not in the condensate.

As for the condensate wavefunction we see an interesting phenomenon: Although the density profile associated with the condensed part of the one-body density matrix is close to that of the trap ground state, the condensate wavefunction is in fact not stationary. The atoms have condensed into a state more resembling a squeezed state[1] and if the incoupling is stopped the wavefunction widths show an oscillating behavior. In Fig. 4 we show $\langle \hat{x}^2 \rangle$ and $\langle \hat{p}^2 \rangle$ of the condensate wavefunction as a function of time. We see that at $\omega t = 2.4$ when the incoupling is stopped, the wavefunction is too wide in momentum space as compared to the ground state of the trap ($\langle \hat{p}^2 \rangle > 1/2$).

One way to avoid this oscillation is to apply δ-kick cooling [23] to the system. This procedure is efficient if there is a linear correlation between position and momentum. In the original suggestion the correlation between position and momentum is brought about by free expansion, but an examination of the condensate wavefunction shows that we have a similar correlation here. The idea is to apply a tight, harmonic trapping potential for a short time interval. If this interval is so short that any changes in position can be ignored, the effect is simply a momentum kick also varying linearly with position. Ideally, this kick brings all the particles to rest. In Fig. 4 we demonstrate that the procedure is effective in our problem. The results are shown for $g = 0$, but a similar reduction is achieved for non-vanishing g.

3.3 The second order correlation function $g^{(2)}(x, y)$

More detailed information about the quantum state of the system is desired and available, and a natural quantity to consider is the second order correlation function

$$g^{(2)}(x,y) \equiv \frac{\langle \hat{\psi}^\dagger(x)\hat{\psi}^\dagger(y)\hat{\psi}(y)\hat{\psi}(x)\rangle}{\langle \hat{\psi}^\dagger(x)\hat{\psi}(x)\rangle\langle \hat{\psi}^\dagger(y)\hat{\psi}(y)\rangle}. \tag{32}$$

It measures the probability to find two atoms at positions x and y normalized to the single-particle densities at the two positions. For a thermal state $g^{(2)} = 2$ while for a coherent state $g^{(2)} = 1$.

As $g^{(2)}$ involves the expectation value of a product of four field operators we are faced with similar factorization problem as when we derived the R&S equations. Again we will resort to the Wick prescription although it should be realized that this is only exact for states obtained with $g = 0$.

We have already evaluated the expectation in the enumerator of Eq.(32) in terms of R and S in the gaussian case. This was done in Eq.(18) and we get for the second order correlation function

$$g^{(2)}(x,y) = 1 + \frac{|R(x,y)|^2 + |S(x,y)|^2}{R(x,x)R(y,y)}. \tag{33}$$

In contrast with the R&S equations the P_+ method has no problems handling expectation values like the enumerator of Eq.(32), and $g^{(2)}$ can be determined exactly up to sampling errors. At relatively short times and low atom numbers we have therefore an excellent tool to obtain exact results even for $g \neq 0$.

[1] This position-momentum squeezing should not be confused with the the atom-field squeezing discussed later.

In Fig. 5 we show a plot of $g^{(2)}(0,0)$ as a function of time for various values of g. The central value slightly above 3 indicates a strong bunching effect where two atoms are more likely to be found close together than in a coherent or a thermal state. This result can be compared with the analytical expression for a single mode squeezed state, generated by the Hamiltonian $\beta\left(\hat{a}^2+\hat{a}^{\dagger 2}\right)$:

$$g^{(2)}=\frac{\langle\hat{a}^\dagger\hat{a}^\dagger\hat{a}\hat{a}\rangle}{\langle\hat{a}^\dagger\hat{a}\rangle^2}=3+\frac{1}{\langle\hat{a}^\dagger\hat{a}\rangle} \tag{34}$$

In the figure we plot both results of the R&S equations using Eq.(33) and the exact P_+ results. Good agreement is found between the two approaches until $\omega t\cong 2.5$ and hereafter the R&S equations fail to capture a decrease in the value of $g^{(2)}$. This decrease indicates a threshold effect that we will discus in the next section.

3.4 Threshold effect

In the semi-classical treatments of the laser and of the parametric oscillator, one identifies a threshold in the stationary balance between gain and loss; the fields shift from fluctuations around zero to fluctuations around finite intensities [24]. Above threshold these optical systems have smaller relative fluctuations of the intensity, and it is natural to expect a similar threshold behaviour in our model. There is a seemingly important difference between our model and the optical systems in the fact that we do not have an explicit dissipative mechanism. It has been known for a long time, and it has been demonstrated explicitly for a large number of physical systems, however, that quite generically, the interactions in many-body systems lead to ergodicity of eigenstates and a dynamical relaxation without coupling to an external bath. For a recent review, see [25].

The R&S equations with their underlying assumption of a gaussian Wigner distribution, centered around vanishing atomic field, are clearly unable to describe correctly the system around and above threshold, but the P_+ simulations are exact, and the discrepancy between the two methods is thus most likely explained by a threshold effect. To investigate more closely the threshold hypothesis, we show in Fig. 6 scatter plots of $\psi_2(0)\psi_1(0)$ at $\omega t=2.4$, 3.0 and 3.6 for a situation with $g=0.02$. From photodetection theory we can deduce the following expression for the atom number distribution

$$P_n(t)=\overline{\frac{[\int\psi_2(x,t)\psi_1(x,t)dx]^n}{n!}\exp\left(-\int\psi_2(x,t)\psi_1(x,t)dx\right)}. \tag{35}$$

This expression, however, exhausts the statistical precision of the P_+ method, since it involves higher moments of the simulated amplitudes, which yield larger and larger fluctuations. Instead, we heuristically present histograms in the figures of how the real parts, $\mathrm{Re}(\psi_2(0)\psi_1(0))$ are distributed, and these histograms are in good qualitative agreement with our picture of a bifurcation of the solution when we reach threshold in the process. It is seen how the distribution at $\omega t=2.4$ is strongly peaked at zero with an exponential tail along the the real axis. At $\omega t=3.0$ this tail extends to larger values, and a shoulder around 120 atoms/a_0 starts to appear, and at $\omega t=3.6$ a second maximum has developed. This explains the lowering of $g^{(2)}$ seen in Fig. 5.

4 Application of a squeezed condensate

In this section we analyse a possible application of the state created in our model. We show how its peculiar statistical properties can be utilized to produce precise measurements. Our suggestion is in direct analogy with the use of a *squeezed vacuum* in quantum optics experiments with beam-splitters. When a beam in such an experiment is incident on a 50/50 beam-splitter and is split in two, the analysis of the noise properties (quantum fluctuations) of the two daughter beams depends crucially on realizing that the incoming beam is not only split at the beam-splitter, it is actually mixed with vacuum coming in from the back-side of the mirror. By replacing this vacuum by a squeezed state we may control the statistical properties of the daughter beams.

The matter wave analogue of the beam-splitter could in our case be a laser pulse which is able to coherently change the internal state of atoms. Such a pulse can drive each atom into a superposition of two internal states.

Suppose now that we have two internal states of the atoms, state a and state b, and that we apply a $\pi/2$-pulse. We then have in the Heisenberg picture

$$\hat{\psi}_a \rightarrow \hat{\psi}'_a = \frac{1}{\sqrt{2}}\left(\hat{\psi}_a + \hat{\psi}_b\right) \tag{36}$$

$$\hat{\psi}_a \rightarrow \hat{\psi}'_b = \frac{1}{\sqrt{2}}\left(\hat{\psi}_a - \hat{\psi}_b\right). \tag{37}$$

The total number operators of atoms in state a and state b after the pulse are thus given by

$$\begin{aligned}\hat{N}'_a &= \int dx \hat{\psi'}^{\dagger}_a(x)\hat{\psi}'_a(x) \\ &= \frac{1}{2}\hat{N}_a + \frac{1}{2}\hat{N}_b + \frac{1}{2}\int dx \left\{\hat{\psi}^{\dagger}_a(x)\hat{\psi}_b(x) + \hat{\psi}^{\dagger}_b(x)\hat{\psi}_a(x)\right\} \qquad (38)\\ \hat{N}'_b &= \int dx \hat{\psi'}^{\dagger}_b(x)\hat{\psi}'_b(x) \\ &= \frac{1}{2}\hat{N}_a + \frac{1}{2}\hat{N}_b - \frac{1}{2}\int dx \left\{\hat{\psi}^{\dagger}_a(x)\hat{\psi}_b(x) + \hat{\psi}^{\dagger}_b(x)\hat{\psi}_a(x)\right\}. \qquad (39)\end{aligned}$$

We will now concentrate on the *difference* in the number of atoms in the two states,

$$\hat{N}'_a - \hat{N}'_b = \int dx \left\{\hat{\psi}^{\dagger}_a(x)\hat{\psi}_b(x) + \hat{\psi}^{\dagger}_b(x)\hat{\psi}_a(x)\right\}. \tag{40}$$

We will also let $\hat{\psi}_a$ initially describe a large condensate while $\hat{\psi}_b$ describes our photodissociated state. That is, we assume that the photodissociation is to the internal state b, while at the time of the $\pi/2$-pulse these atoms are overlapped with a large normal condensate in the internal state a. The large condensate is assumed to be in a coherent state with a definite phase , *e.g.*

$$\begin{aligned}\hat{\psi}_a(x)|\rangle &= e^{i\theta}\phi_a(x)|\rangle \qquad (41)\\ \langle|\hat{\psi}^{\dagger}_a(x) &= e^{-i\theta}\phi_a(x)\langle| \qquad (42)\end{aligned}$$

with ϕ_a real. The mean number of atoms is given by

$$N_a = \langle\hat{N}_a\rangle = \int dx\ \phi^2_a(x). \tag{43}$$

Using Eq.(40) we find

$$\left\langle \hat{N}'_a - \hat{N}'_b \right\rangle = 0 \tag{44}$$

and

$$\left\langle \left(\hat{N}'_a - \hat{N}'_b\right)^2 \right\rangle = N_a + N_b + \iint dxdy\ \phi_a(x)\phi_a(y)\mathrm{Re}\left[R_b(x,y,) + e^{-2i\theta}S_b(x,y,)\right]. \tag{45}$$

Ordinary vacuum in the b-state is the special case with $S_b = R_b = N_b = 0$ and we note that the typical imbalance of populations is $\sqrt{\mathrm{Var}(N'_a - N'_b)} = \sqrt{N_a}$. Now, we use the nontrivial state created by photodissociation as squeezed vacuum. We imagine to have experimental control over θ and choose this phase optimally in order to reduce $\mathrm{Var}(N'_a - N'_b)$.

In Fig. 7 we plot this minimum value of $\mathrm{Var}(N'_a - N'_b)/N_a$ as a function of the time of production of the squeezed condensate. It is clearly seen how the noise is rather quickly suppressed almost perfectly. In the particular case shown N_a was taken to be 10^3 and ϕ_a was of gaussian shape. The

time-dependent number of atoms in the b-condensate can be approximately read out of Fig. 2. The width of ϕ_a was chosen to be the same as the equilibrium width of the b-state atoms. It is amazing, but of course already well-known in quantum optics, that this supression can take place even though the number of atoms initially in the b-state is very small compared to the average number of atoms in the large condensate in the a-state

At times beyond $\omega t \cong 2$ the noise suppression is lost in the exact P_+ simulations. We recall that for $g = 0$, the R&S equations are exact, and it is thus natural to ascribe the discrepancy between the two methods to the interactions, which, by analogy with the Kerr-effect in optics, cause a deformation of the gaussian state. In Fig. 8 we show a scatter plot of the amplitudes of the projections, ψ_{1a}, of 3000 P_+ realizations of ψ_1 on ϕ_a at $\omega t = 2.4$ for $g = 0.00$ and for $g = 0.02$. Such plots should be interpreted with care, as in general the *pair* (ψ_1, ψ_2) is needed to calculate all normal-ordered expectations. The Kerr-effect, however, influences the S-function, and to calculate $\langle \hat{\psi}^2 \rangle$ we only need to average ψ_1^2. In our case the relevant contributions to this average can thus be depicted by a scatter plot of ψ_{1a} alone.

We see in Fig. 8a a gaussian state represented by points which form an ellipse-like structure. If the distibution had no prefered direction in phase-space $\langle \hat{\psi}^2 \rangle = \overline{\psi_1^2}$ would vanish, but this is clearly not the case for our squeezed state. In Fig. 8b the the interaction modifies the phase accumulation of points with large values of $|\psi_1|$ and deforms the distribution to an S-like shape, and the mean value of ψ_1^2 is reduced. If the state is centered around a finite field amplitude, the intensity dependent phase shift transforms a circular distribution into a bean-shaped one, and in that case the Kerr effect actually produces squeezing [26].

5 Discussion

In this paper we have studied the matter wave analogue of an optical parametric oscillator. We have developed a description based on the correlations of the atomic field and we have supplemented this by the P_+ method. When interactions are taken into account both treatments were limited to relatively short times and low numbers of atoms. We showed how the state can be used as squeezed vacuum to improve the statistics of experiments with larger condensates.

On the theoretical side, it is of course interesting to remedy the breakdown of the R&S method as we know that for large condensates an even simpler description, the Gross-Pitaevskii equation, is very successful. To bridge the gap between the two regimes which are both describable in simple terms would be interesting and could be useful also in other scenarios where special quantum states of a BEC are created. In such work it is very likely that time dependent Monte Carlo methods, based for example on the positive P distribution, P_+, will play a significant role.

Let us finish this paper with a brief mentioning of other proposals for the preparation of quantum correlated atomic condensates. As mentioned in the introduction, the collisional interaction has been proposed as an agent for the preparation of quantum correlated states, such as Schrödinger cat-like states [7]. The states prepared by our proposal are substantially less 'non-classical', but provided the existence of a molecular condensate, we believe that the experimental requirements of our proposal are more easy to meet.

It was suggested some time ago to prepare spin-squeezed states of non-degenerate atomic gasses and of trapped ions [27], and concrete proposals were made, involving coupling of the atoms *via* their interaction with a quantized field mode [28], or their center-of-mass motion [29]. More recently, it was suggested, and experimentally proven possible, to induce transitions between atomic states in an optically thick sample by absorption of non-classical light, and thereby to transfer quantum correlations from the light field to the atoms [30]. Ingredients of these proposals become even more powerful with cavities around the samples [31]. Very promising, recent ideas are based on quantum non-demolition (QND) measurements of, *e.g.*, quadratures or populations in the atomic sample by refraction of light beams. Such detection suffices to establish quantum correlations in the sample, even though the detection is done with classical field states [32]. One may simply use the state following the QND measurement together with the known classical outcome of the measurement to perform subsequent high-precision experiments, or one may consider

feed-back loops, in which the system is driven towards a specific quantum correlated state.

All of these proposals are also relevant for degenerate gasses. The QND methods are probably closest to real implementation, since phase contrast methods, already used for imaging of condensates in many experiments, only have to be carried out with properly chosen parameters to lead to quantum correlated atomic states. But all methods are interesting, and they may illuminate various aspects of the condensate dynamics, as illustrated, *e.g.* by the threshold phenomenon and the 'Kerr-effect' suppression of squeezing in the proposal in this paper.

Synthesis of correlated noise

In order to numerically simulate Eqs.(23,25) we discretize time and space, and we synthesize noise terms, $dW_{1,2}(x_n,t_i)$, that obey discretized versions of Eqs.(26-29). It is well-known how independent (pseudo) random numbers from different distributions can be created. For example a Gaussian distribution can be created starting from uniformly distributed numbers *via* the Box-Müller method, *i.e.* we know how to produce $\{dU_{1,2}(x_n,t_i)\}$ so that

$$\langle dU_{1,2}(x_n,t_i)\rangle = 0 \tag{46}$$

$$\langle dU_\alpha(x_n,t_i)dU_\beta(x_m,t_j)\rangle = \delta_{\alpha\beta}\delta_{nm}\delta_{ij}. \tag{47}$$

We see that the correlation functions, Eqs.(28,29), contain two terms: one from the interaction and one from the incoupling. These can be treated separately if we split the noise in two independent contributions

$$dW_{1,2}(x_n,t_i) = dW^g_{1,2}(x_n,t_i) + dW^b_{1,2}(x_n,t_i) \tag{48}$$

Due to the contact form of the interaction, the corresponding noise term poses no difficulties; we simply choose

$$dW^g_{1,2}(x_n,t_i) = \sqrt{\frac{\pm ig\psi(x_i)dt}{dx}}dU^g_{1,2}(x_n,t_i), \tag{49}$$

where $dU^g_{1,2}$ is chosen with the properties (46,47). The incoupling term is created by multiplication and convolution of uncorrelated noise $dU^b_{1,2}$ of the form (46,47) with suitable Gaussian functions:

$$dW^b_{1,2}(x_n,t_i) = \mathcal{N}\exp\left(\pm it_i\Delta\right)\exp\left(-\frac{x_n^2}{2\sigma_a^2}\right)\sum_{n'}dx\; dU^b_{1,2}(x_{n'},t_i)\exp\left(-\frac{(x_n-x_{n'})^2}{2\sigma_b^2}\right) \tag{50}$$

It turns out that choosing

$$\sigma_a^2 = 2\sigma_{cm}^2, \qquad \sigma_b^2 = \frac{2\sigma_{cm}^2\sigma_r^2}{4\sigma_{cm}^2-\sigma_r^2}, \qquad \mathcal{N} = \sqrt{\frac{\pm idtB}{dx\sqrt{\pi}\sigma_r\sigma_{cm}\sigma_b}} \tag{51}$$

is sufficient to fulfill Eq.(26) with b given by Eq.(7). σ_r and σ_b are rather small, and in practice the sum in Eq.(50) only needs to involve a few terms.

References

[1] C. S. Adams, M. Sigel, and J. Mlynek, Physics Reports **240**, 143 (1994); *Atom Interferometry* ed. by P. Berman (Academic Press, 1997); *Nanomanipulation of atoms*, D. Mensched and J. Mlynek (eds.), Special issue of Appl. Phys. B **70**, 649-730 (2000).

[2] M. R. Andrews *et al.*, Science **275**, 637 (1997).

[3] E. W. Hagley *et al.*, Phys. Rev. Lett. **83**, 3112 (1999).

[4] S. Inouye *et al.*, Nature **402**, 641 (1999)

[5] C. Fabre and E. Giacobino (eds.), *Quantum Noise Reduction in Optical Systems*, Special issue of Appl. Phys. B **55** (1992).

[6] L. Deng *et al.*, Science **398**, 218 (1999).

[7] J. I. Cirac, M. Lewenstein, K. Mølmer, and P. Zoller, Phys. Rev. A, **57**, 1208 (1998);D. Gordon and C. M. Savage, Phys. Rev. A. **59**, 4623 (1999).

[8] G. J. Milburn, J. Corney, E. M. Wright and D. W. Walls, Phys. Rev. A **55**, 4318 (1997); S. Raghavan, A. Smerzi, S. Fantoni and S. R. Shenoy, cond-mat/9706220; A. Smerzi, S. Fantoni, S. Giovanazzi and S. .R. Shenoy, cond-mat/9706221.

[9] S. Inouye it et al., Nature **392**, 151 (1998);S. L. Cornish *et al.*, cond-mat/0004290.

[10] M. Mackie, R. Kowalski, and J. Javanainen, Phys. Rev. Lett. **84**, 3803 (2000).

[11] R. Wynar *et al.*, Science **287**, 1016 (2000).

[12] D. J. Heinzen, R. Wynar, P. D. Drummond, and K. V. Kheruntsyan, Phys. Rev. Lett. **84**, 5029 (2000);C.-Y. Lin, M. S. Hussein, A. F. R. de Toledo Piza, and E. Timmermans, cond-mat/9911247;M. Holland, J. Park, and R. Walser, cond-mat/0005062.

[13] P. D. Drummond, K. V. Kheruntsyan, and H. He, Phys. Rev. Lett. **81**, 3055 (1998).

[14] K. Huang, *Statistical Mechanics*, 2 ed. (John Wiley & Sons, Singapore, 1987).

[15] M. J. Steel *et al.*, Phys. Rev. A **58**, 4824 (1998).

[16] M. Edwards *et al.*, J. Phys. B: At. Mol. Opt. Phys. **32**, 2935 (1999);N. Robins, C. Savage, and E. Ostrovskaya, cond-mat/0004127 (2000).

[17] M. Kitamura and T. Tokihiro, J. Opt. B: Quantum Semiclass. **1**, 546 (1999).

[18] C. W. Gardiner, *Quantum Noise* (Springer-Verlag, Berlin Heidelberg, 1991).

[19] K. Huang, *Quantum Field Theory* (John Wiley & Sons, New York, 1998).

[20] P. D. Drummond and J. F. Corney, Phys. Rev. A **60**, R2661 (1999).

[21] I. Carusotto, Y. Castin, and J. Dalibard, cond-mat/000399.

[22] A. M. Smith and C. W. Gardiner, Phys. Rev. A **39**, 3511 (1989);A. Gilchrist, C. W. Gardiner, and P. D. Drummond, Phys. Rev. A **55**, 3014 (1997).

[23] H. Ammann and N. Christensen, Phys. Rev. Lett. **78**, 2088 (1997);S. H. Myrskog *et al.*, Phys. Rev. A **61**, 053412 (2000).

[24] Laser Physics, M. Sargent III, M. O. Scully, and W. E. Lamb (Addison Wesley, Reading Massachusetts, 1974);L. A. Lugiato, C. Oldano, C. Fabre, E. Giacobino, and R. J. Horowicz, Nuovo Cimento **D 10**, 959 (1988).

[25] T. Guhr, A. Müller-Groeling, and H. A. Weidenmüller, Phys. Rep. **299**, 189 (1998).

[26] S. Reynaud, C. Fabre, E. Giacobino, and A. Heidemann, Phys. Rev. A **40**, 1440 (1989).

[27] M. Kitagawa and M. Ueda, Phys. Rev. A **47**, 5138 (1993);D. J. Wineland *et al*, Phys. Rev. A. **50**, 67 (1994).

[28] G. S. Agarwal and R. R. Puri, Phys. Rev. A **41**, 3782 (1990).

[29] D. J. Wineland *et al*, Phys. Rev. A **46**, R6797, (1992); K. Mølmer and A. Sørensen, Phys. Rev. Lett. **82** 1835-1838 (1999);A. Sørensen and K. Mølmer, Phys. Rev. Lett. **83**, 2274 (1999)

[30] A. Kuzmich, K. Mølmer, and E. Polzik, Phys. Rev. Lett. **79**, 4782-4785 (1997);J. Hald, *et al*, Phys,. Rev. Lett. **83**, 1319 (1999); A. E. Kozhekin, K. Mølmer, and E. Polzik, To appear in Phys. Rev. A

[31] M. Fleischhauer *et al.*, quant-ph/9912046.

[32] A Kuzmich, *et al*, Europhys. Lett. **42**, 481 (1998); Phys. Rev. A. **60**, 2346 (1999); K. Mølmer, Eur. Phys. J. **D 5**, 301 (1999); Y. Takahashi *et al*, Phys. Rev. A. **60**, 4974 (1999); A. Kuzmich and E. S. Polzik, quant-ph/0003015; Lu-Ming Duan, J.I. Cirac, P. Zoller, E. S. Polzik, quant-ph/0003111.

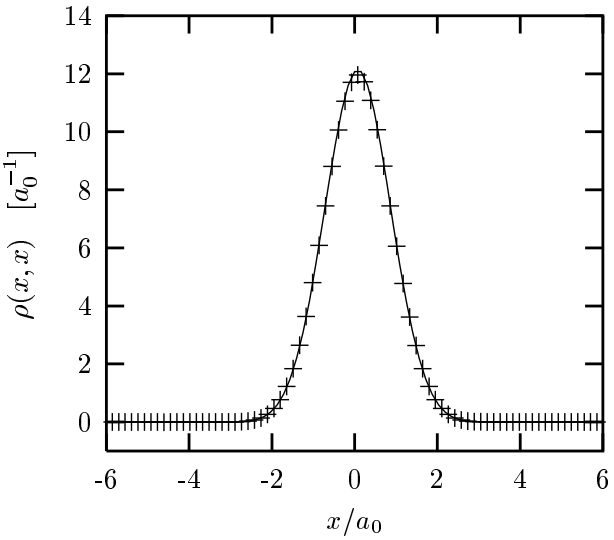

Figure 1: The density profile at time $\omega t = 2.4$ for interaction strenght $g = 0.01$ and incoupling parameters $B = 3.0\hbar^2/m$, $\Delta = \omega$, $\sigma_{cm} = a_0$ and $\sigma_r = 0.2a_0$. The solid curve shows the results of the coupled R&S equations, the crosses are obtained with the P_+ simulations.

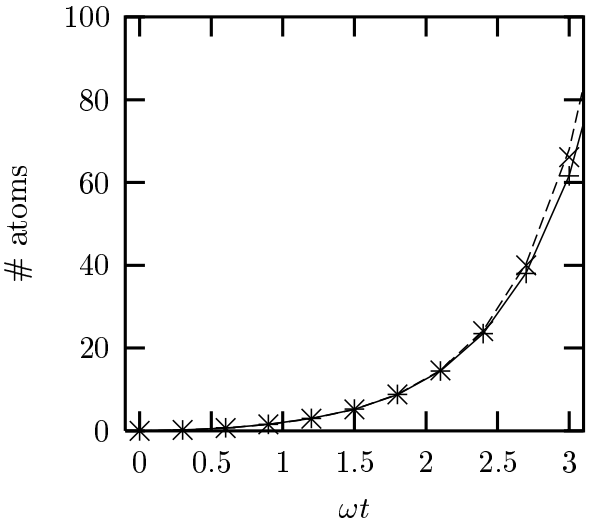

Figure 2: The number of photo-dissociated atoms as a function of time. The solid and dashed curves show the results of the R&S equations for $g = 0.00$ and $g = 0.01$ while the symbols + and $\times$ indicate the corresponding results of the P_+ Langevin equations. Incoupling as in Fig.1.

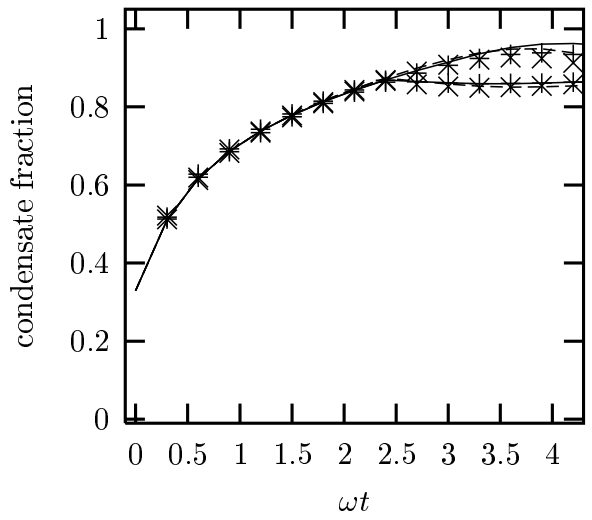

Figure 3: The condensate fraction, *i.e.*, the ratio of the largest eigenvalue of the one-body density matrix to the total number of atoms (trace of the one-body density matrix). Solid and dashed curves shown the results of the R&S equations for $g = 0.01$ and for $g = 0.02$. The corresponding results of the P_+ simulations are indicated by the symbols + and $\times$. The lower sets of data with the same symbols show the results when the incoupling is stopped at $\omega t = 2.4$.

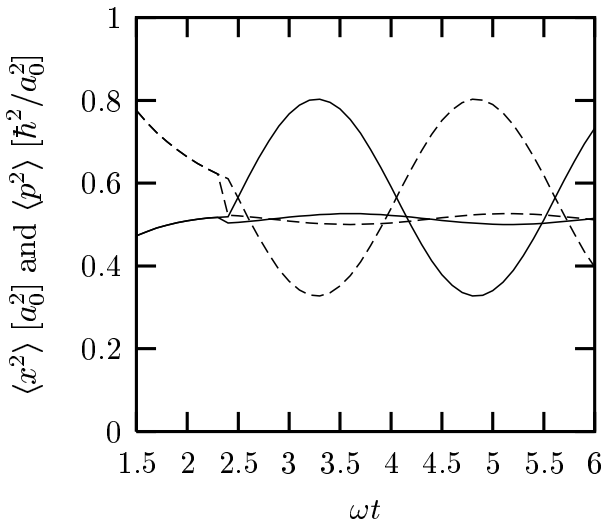

Figure 4: The freely evolving expectation values of $\langle x^2\rangle$ (solid curve) and $\langle p^2\rangle$ (dashed curve) are compared to the results obtained after application of a δ-kick to match the wavefunction with the ground state in the trap. If we apply a properly chosen kick just as we stop the incoupling at $\omega t = 2.4$ the oscillations can be almost completely removed.

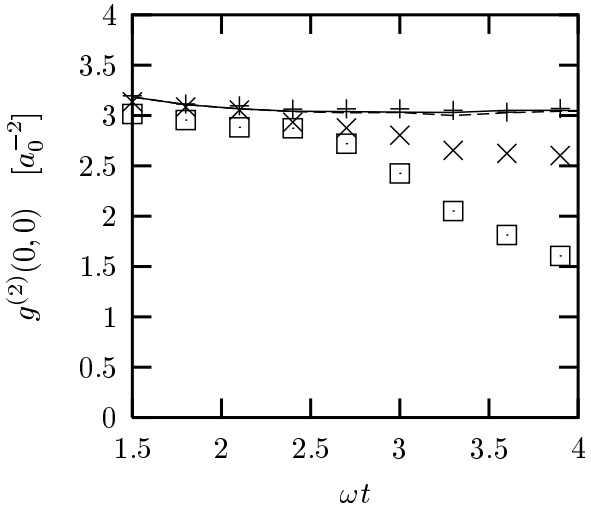

Figure 5: The second order correlation function $g^{(2)}(x,y)$ evaluated at $y = x = 0$ as a function of time. The solid and dashed lines show the results of the R&S equations for $g = 0$ (exact) and $g = 0.02$. The symbols + and $\times$ show the results of the P_+ simulations with $g = 0.00$ and $g = 0.02$. The photo-dissociation stops at $\omega t = 2.4$. For $g \neq 0$, here is a strong discrepancy between the results of the R&S equations and the P_+ at times beyond $\omega t = 2.5$. The effect is clearly dependent on the interaction. The symbol $\boxdot$ show P_+ results obtained when $g = 0.02$, and when the photodissociation is not interrupted.

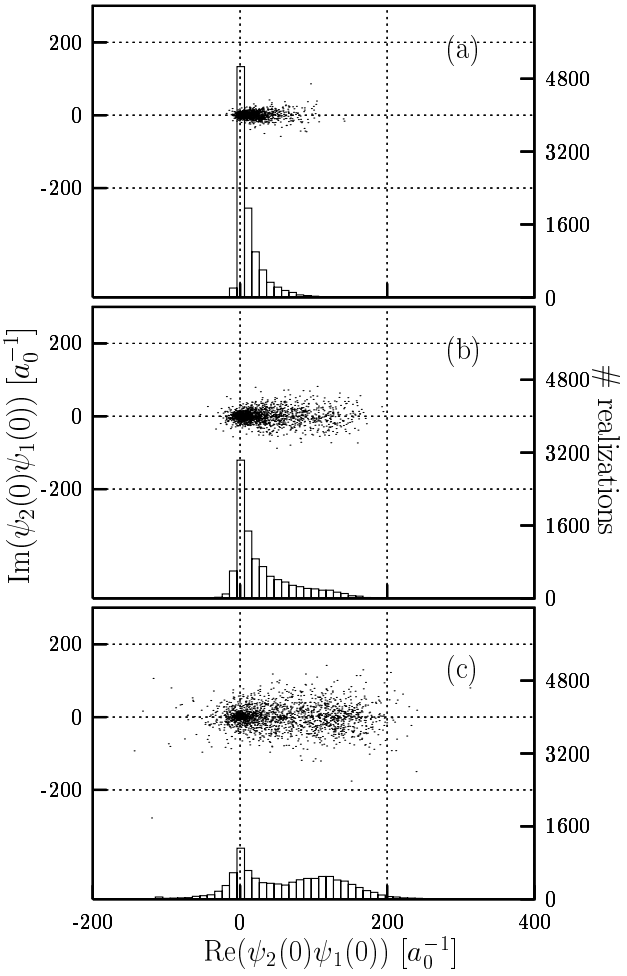

Figure 6: Scatter plots of $\psi_2(0)\psi_1(0)$ from the P_+ realizations for $\omega t = 2.4$ (a), $\omega t = 3.0$ (b), and $\omega t = 3.6$ (c). The average of this quantity is $\langle\hat{\psi}^\dagger(0)\hat{\psi}(0)\rangle$, the central density in the trap and higher order, normally ordered, moments $\langle\hat{\psi}^{\dagger n}\hat{\psi}^n\rangle$ are similar averages $\overline{(\psi_2(0)\psi_1(0))^n}$. For clarity, we show in the bottom of the plots histograms of $\mathrm{Re}(\psi_2(0)\psi_1(0))$. It is seen how the character of the state changes with time as a second maximum in the distribution develops at a value different from zero.

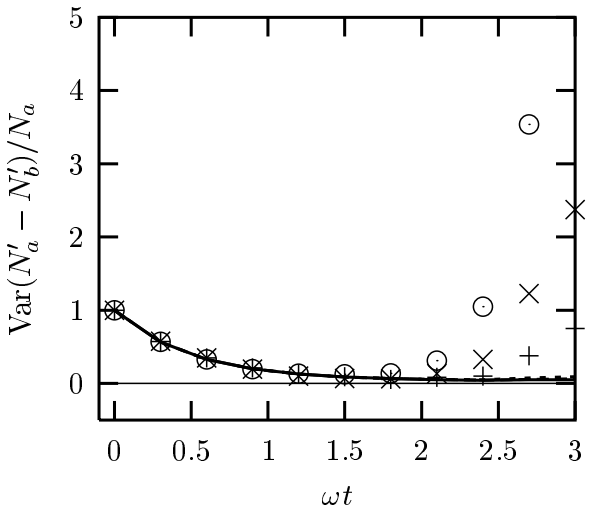

Figure 7: The minimum value of $\mathrm{Var}(N'_a - N'_b)/N_a$ as a function of the time of application of the $\pi/2$-pulse. All data are for a situation where incoupling is stopped at $\omega t = 2.4$. Calculations were done with three different interaction strengths ($g = 0.005$, 0.01 and 0.02) and the almost overlapping lines (solid, dashed and dotted) show the results of R&S equations while the symbols ($+$, $\times$ and $\odot$) show the results of the P_+ simulations.

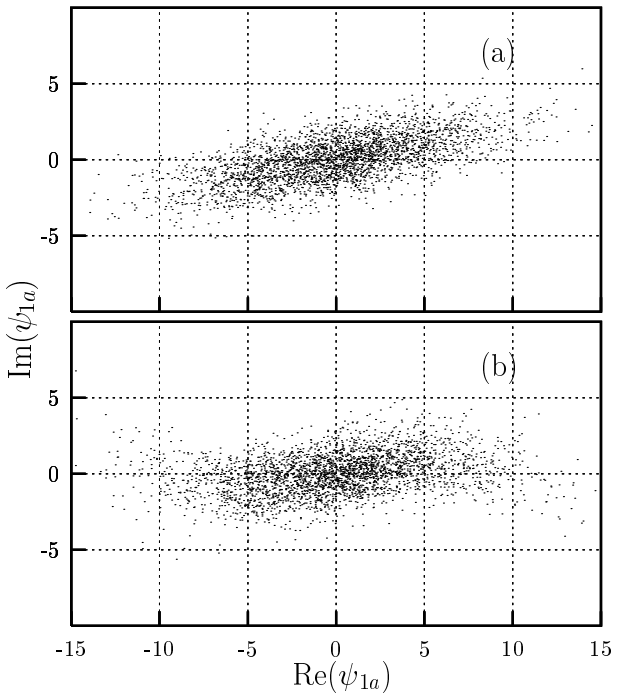

Figure 8: Scatter plots of ψ_{1a}, the overlap of ψ_1 with the condensate mode function $\phi_a/\sqrt{N_a}$. Plot (a) is for $g = 0.00$ while plot (b) is for $g = 0.02$. The plots demonstrate the deforming effect of the interactions on the gaussian state. This deformation reduces the mean of ψ_{1a}^2 which is the decisive factor for the efficiency of the state as squeezed vacuum.